



**OTC-35570-MS**

## **Enabling Resident AUV and ROV Subsea Operations: The Role of Wireless Inductive Charging and Docking Stations**

T. J. J. Meyer, H. Mubasier, and K. T. Humborstad, Unplugged, Kristiansand, Agder, Norway; H. S. Eide, Subsea USB, Sandnes, Rogaland, Norway; A. Vasilijevic, Norges Teknisk Naturvitenskapelige Universitet, Trondheim, Trøndelag, Norway; J. C. Torvestad, Equinor, Stavanger, Rogaland, Norway

Copyright 2025, Offshore Technology Conference DOI [10.4043/35570-MS](https://doi.org/10.4043/35570-MS)

This paper was prepared for presentation at the Offshore Technology Conference held in Houston, TX, USA, 5 – 8 May, 2025.

This paper was selected for presentation by an OTC program committee following review of information contained in an abstract submitted by the author(s). Contents of the paper have not been reviewed by the Offshore Technology Conference and are subject to correction by the author(s). The material does not necessarily reflect any position of the Offshore Technology Conference, its officers, or members. Electronic reproduction, distribution, or storage of any part of this paper without the written consent of the Offshore Technology Conference is prohibited. Permission to reproduce in print is restricted to an abstract of not more than 300 words; illustrations may not be copied. The abstract must contain conspicuous acknowledgment of OTC copyright.

---

### **Abstract**

This paper explores the potential of wireless inductive charging technology, enabling the deployment of Subsea Docking Stations (SDS) as a cornerstone for the operation of resident autonomous underwater drones. A notable milestone was achieved in 2023 at Equinor's Njord Field in the North Sea, where an SDS facilitated a world-record 165-days continuous operation of an underwater drone. The drone successfully docked and undocked 280 times on the SDS inductive chargers to recharge its batteries and transfer mission data, establishing itself as a fully operational resident system. This breakthrough highlights the key role of inductive technology as an enabler of continuous autonomous subsea operations.

The core success of the subsea docking station presented in this article stems from its foundation in open innovation and collaborative standardisation, which are essential for establishing a fully interoperable subsea ecosystem. Drawing inspiration from a land-based gas station—where any vehicle, irrespective of brand, can refuel seamlessly—the SDS achieves interoperability and compatibility across multiple drone types and manufacturers. This is made possible by integrating advanced yet standardised inductive charging technology, enabling wireless transfer of both power and data.

Beyond the offshore energy sector, this paper examines how inductive charging stations, initially designed for oil and gas applications utilising work-class Remotely Operated Vehicles (ROVs), are being reimagined and adapted to support charging and docking of micro-drones, i.e. Autonomous Underwater Vehicles (AUVs), in emerging markets such as aquaculture. The advancement of compact inductive SDS exemplifies the flexibility of this technology and highlights the growing demand for standardised inductive docking solutions across a wide range of applications.

### **Introduction**

Driven by increasing demand for continuous subsea presence, traditional remotely operated vehicle (ROV) and autonomous underwater vehicle (AUV) operations, constrained by surface vessel dependency and weather limitations, are being revolutionised through the introduction of subsea docking stations (SDS).

SDS enable AUVs and ROVs, categorised as Underwater Intervention Drones (UIDs) in this paper, to recharge and transfer data without surfacing; henceforth, SDS technology reduces reliance on surface vessels and human intervention. The technology unlocks (i) reduced costs, (ii) increased operational safety and (iii) a positive impact on the environment.

- i. Classical ROV missions involve costs associated with ROV services, support vessel expenses, and additional equipment. Approximate daily rates for ROV operations at depths of 200 to 1,000 meters are approximately \$40,000 per day, while operations beyond 1,000 meters can cost around \$60,000 per day, though current rates are higher as these figures are based on 2018 data (Tillin, 2018). Diving Support Vessels (DSV), integral to deep-water ROV deployments, have seen charter rates averaging \$150,000 per day in late 2023 (Martyn Wingrov, 2023). ROV mission durations vary widely, from 1 to 3 days for inspection or maintenance tasks to several weeks or months for complex construction support or scientific research operations. Overall, without factoring in additional costs such as specialised equipment integration (e.g., sonar systems), depending on the operating depth, ROV mission costs typically range between \$50,000 to \$250,000+ per day. In the context of offshore oil and gas fields, where power and data infrastructure are already built for 30+ years of operational lifetime, introducing an SDS at a capital cost of \$1–2 million presents a compelling business case as a cost-effective alternative to repeated ROV missions especially if the end users plan to own UIDs fleets where the vehicles can be transferred from one field to another.
- ii. The operational limits of ROV missions are significantly influenced by sea state conditions; for example, DNV recommended practices suggest a limit of 2.5m significant wave during the critical phases of ROV launch and recovery (Magnus Valen, 2010). In contrast, resident underwater intervention drones, designed for 12-month operations (Ariana Hurtado, 2021) leverage SDS technology to facilitate continuous 24/7 remote operations, independent of weather conditions. For example, in 2023, the resident drone Liberty E-ROV completed 163 missions, logging nearly 14,000 operational hours. This approach eliminated approximately 10,000 hours of support vessel usage, reduced 240 personnel crew changes typically required for 12-hour shifts over 14-day rotations, and saved an estimated 400 vessel days (Hurtado, 2023).
- iii. One of the most significant contributions of SDS systems is their alignment with decarbonisation strategies. Conventional inspection, maintenance, and repair (IMR) campaigns with ROV relying on surface vessels emit substantial amounts of carbon dioxide (CO<sub>2</sub>). For example, a 14-day IMR campaign using a conventional DSV will emit approximately 644 metric tons of CO<sub>2</sub>, primarily due to the fuel consumption. In contrast, resident systems such as the Liberty E-ROV, which draw power from battery packs and utilises SDS technology to recharge, emit 178 metric tons of CO<sub>2</sub> over the same period, resulting in a net savings of approximately 466 metric tons of CO<sub>2</sub> (Hurtado, 2023).

Given the advantages listed above, British Petroleum (BP) considered already in 1986, an integrated ROV launch system onboard the subsea oil production system (Elaine Maslin, 2021). However, despite nearly four decades of technological advancements, operational SDS are still a rare sight (Vasilijevic et al., 2023) mainly due to three key aspects: (a) the diverse range of vehicle form factors requires multiple types of docking and charging solutions, (b) achieving efficient power transfer and high-speed data communication in subsea environments continues to present significant technical difficulties (Martínez de Alegría et al., 2024), (c) resident autonomous inspection UIDs are currently capable of performing only limited operations, necessitating the deployment of a crewed vessel for unplanned interventions (Elaine Maslin, 2021).

This paper examines the technological evolution and implementation of the SDS initiative supported by Equinor, currently under testing in the Njord field, with particular focus on how the (a), (b) and (c) points listed above are being addressed via:

- the adoption of an open innovation approach, where Computer-Aided Design (CAD) files for the SDS are made freely available to promote standardisation and collaboration (cf. section 2),
- the adoption of inductive charging technologies aligned with the Subsea Wireless Group (SWiG) standards enhances interoperability and efficiency in power and data transfer (cf. section 3),
- the integration of a tether system connected to the SDS enables UIDs to transition seamlessly between autonomous AUV and remotely operated ROV modes (cf. section 4)

## The Subsea Docking Station (SDS), a Standardised and Open Innovation

The SDS concept reviewed in the remainder of this publication is based on the initiative supported by Equinor in collaboration with Blue Logic, Unplugged and Subsea USB. In this concept, the SDS provides a cost-effective mean for any UID to dock, recharge and upload or download data at depths up to 3000m (Fig. 1).



Figure 1—(left) Traditional ROV operation compared to resident UID operation, (right) SDS concept visualisation, a docked UID recharging and transferring data.

The SDS concept is anchored around the following four main concepts:

- Open innovation:** The CAD files for the steel components of the Subsea Docking Station (SDS) (yellow parts in Fig. 1) are freely accessible. While the SDS is primarily designed as a landing platform, its modular architecture allows for the addition of supplementary structures, enabling compatibility with torpedo-style drones.
- Modularity:** To enhance the operational flexibility and avoid vendor lock-in, the charging station subsea control module (SCM) interconnecting the SDS with the subsea infrastructure and its consumers (i.e. inductive couplers used for charging drones or powering sensors) is an independent electronic module that adopts an Internet of Things (IoT) architecture akin to terrestrial systems. This ensures that the SDS operates independently of the Subsea Production System (SPS) network, thereby facilitating seamless network integration. Furthermore, the power design of the SCM accommodates a broad range of input voltages, including AC voltages from 110 to 3000 VAC, ensuring compatibility with existing brownfield infrastructures as well as 400 VDC inputs, aligning with the Direct Current Fiber Optic (DCFO) systems utilised in new fields. The charging station SCM also supports Uninterrupted Power Supply (UPS) functionality and provides CAN open interfacing with external battery systems to enhance operational flexibility and reliability in various subsea environments.
- Standardisation:** The chosen method for charging underwater intervention drones utilises inductive couplers that align with the standards established by SWiG. This standardisation will establish full interoperability across mechanical, data, and power interfaces between the primary and secondary sides of inductive couplers, regardless of their manufacturer.

- Durability:** The SDS is engineered for a robust operational lifespan of 30 years, with its inductive couplers, which have the inductive interface directly exposed to seawater, designed to achieve a minimum service life of 15 years. The engineering adheres to the manufacturing guidelines API Standard 17F (API 17F, 2023) and Equinor's Technical Requirement TR1231, Appendix D (Sirevaag & Rettedal, 2021).

This open and standardised innovation has been thoroughly experimented with. In 2019, three SDSs were built, and each one has been successfully demonstrated and tested with underwater vehicles. These tests were conducted at multiple locations, including: (i) the SAAB Test Center in Sweden, where the SAAB Seaye Sabertooth autonomous underwater vehicle was utilised; (ii) Saipem's Test Center in Trieste, Italy, featuring the Hydrone-R UID, and (iii) the Tau Test Center near Stavanger, Norway, which involved the Oceaneering Freedom pilot vehicle, Eelume's M-series snake-shaped drone, and the Stinger UID. Three docking stations are currently permanently installed, and in operations, those are in the Trondheimsfjorden for use by the Norwegian University of Science and Technology (NTNU) (Vasilijevic et al., 2023), Tau Test Center and the Njord field operated by Equinor. Two more SDS are ready for deployment at the Johan Castberg and Åsgard fields.

New deployments are currently being considered at Johan Castberg, Snøhvit, Askeladd, Aasta Hansteen, Norne, Heidrun, Gullfaks, Troll, Snorre, Oseberg, Grane (Breidablikk) and Sleipner positioning the SDS as the most widely adopted subsea docking solution to date (Fig. 2). Furthermore, prominent underwater drone manufacturers, including Oceaneering, Saipem, and SAAB, have incorporated SWiG inductive compliant couplers into their designs, ensuring that multiple drone models are compatible with and capable of docking on the SDS infrastructure (Fig. 3).



Figure 2—SDS current planned and considered deployments



Figure 3—Oceaneering, Saipem, and SAAB UIDs interface on the SDS

### Mechanical Overview of the Subsea Docking Station (SDS)

Mechanically, the SDS consists of two main components: the Subsea Docking Base (SDB) and the Subsea Docking Module (SDM) (see Fig. 4). The SDB serves as a robust structural platform designed to securely support the SDM on the seabed. It interfaces with various foundation systems, such as suction anchors (as illustrated in Fig. 3), gravity bases, or anchoring to pre-existing structures such as a well slot, providing flexibility in deployment scenarios. To facilitate the installation process, the SDB is equipped with API17D guide funnels at each corner, and the whole SDS assembly can be installed in a single lift via the moonpool (see Fig. 15) at wave height up to 5.5 m or overboard via a lifting crane installed on an offshore support vessel.



Figure 4—The Subsea Docking Station (SDS) consists of two main components: the Subsea Docking Base (SDB) and the Subsea Docking Module (SDM).

The Subsea Docking Module (SDM), with a minimum landing area of 4000×1680 mm, is a recoverable component that serves as the interface between the subsea infrastructure and UID. It houses critical electronic systems, including the subsea control module, batteries, and accommodates all power and data outlets—both conductive and inductive—that facilitate power transfer, data communication, and docking for UIDs. One possible configuration of the SDM is depicted in Fig. 5. The configuration of the consumer outlets is adaptable and field-specific, enabled by the modularity of the SCM, which supports a wide range of arrangements (i.e. up to 8 power and data outlets) to meet various operational requirements (see Fig. 6).

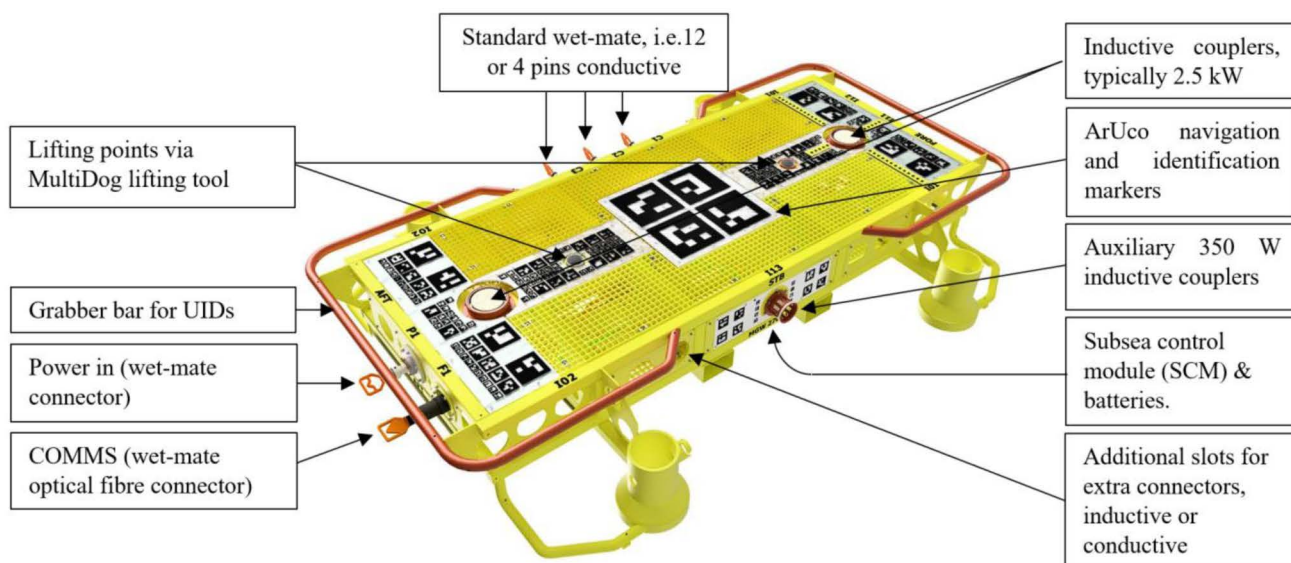


Figure 5—A possible configuration of the SDM with 2.5kW and 350W inductive outlets to charge or tether drones as well as standard wet-mate connectors to power other consumer types such as sensors, subsea modems, etc. The design of the SCM allows for eight power & data consumers to be connected simultaneously.

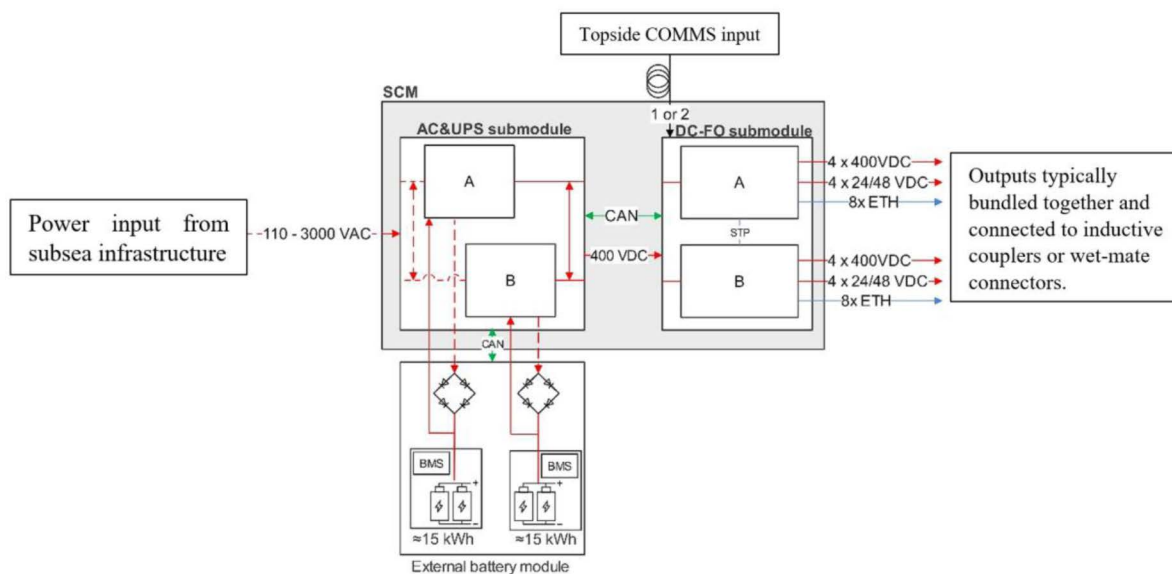


Figure 6—Subsea Control Module block diagram. All the modules, including the battery module, AC&UPS submodule and DC-FO submodule, are housed beneath the charging station, creating a compact, integrated turn-key design.

## 2.2. Modular field configuration via a modular subsea control module

Beneath the SDM top grid lies the subsea control module (see Fig. 7), supporting the interface between the subsea infrastructure and UIDs. The subsea control module, commonly referred to as "junction boxe(s)", consists of vendor-independent canister(s). The details provided in this publication pertain to the Blue Logic SCM; however, it is important to note that other vendors, such as Aker Solutions/Siemens, also offer SDM subsea control modules (Pimentel & Kristiansen, 2022).

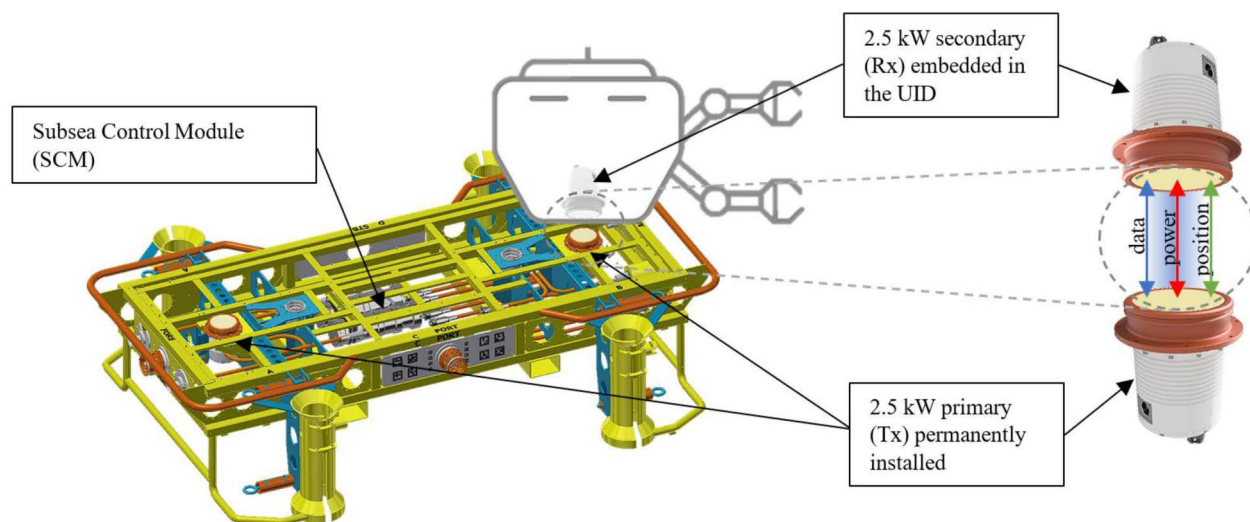


Figure 7—Inductive coupler used in the SDS, the primary side (Tx) is installed in the charging station and the secondary (Rx) in the UID

The subsea electronic module of the subsea docking module is designed to accommodate 400 VDC inputs, ensuring compatibility with Direct Current Fiber Optic (DC-FO) systems; additionally, the SCM supports alternating current (AC) with input voltages ranging from 110 to 3000 VAC, providing interoperability with existing brownfield infrastructures. Recognising the challenges associated with delivering high power in brownfield subsea environments, the SCM is engineered to include Uninterrupted Power Supply (UPS) functionality (see Fig. 6).

To optimise cost-effectiveness and modularity, the SCM is divided into two distinct subsystems: the DC-FO submodule and the AC&UPS submodule. This modular approach allows for flexibility in deployment. In fields equipped with DC-FO infrastructure, only the DC-FO submodule is required. Conversely, in brownfield environments, the AC&UPS submodule can be added with the additional option of connecting an external battery to allow for system deployment when power delivery is limited.

The **DC-FO submodule**, qualified as per API17F, is designed with built-in redundancy, featuring dual A and B sides to enhance reliability. It operates on a 400 VDC input line and establishes communication with the topside network via optical fibre connections. The submodule provides eight galvanically insulated and controlled 400 VDC outlets, each capable of delivering up to 4 kW of power. These outlets are typically utilised to supply power to inductive consumers rated at 96 W (API17F, SIIS Level 3 High Power) up to 2.5 kW or to conductive 4-pin wet-mate connectors. In addition to high-voltage outlets, the DC-FO unit offers eight low-voltage 24 or 48 V outlets supporting up to 240 or 480 W of power, respectively. These outlets are primarily used to power sensors or modems. Furthermore, the submodule is equipped with 16 Ethernet outlets, each delivering a bandwidth of 1 Gbps, facilitating high-speed data communication to the consumers.

The **AC&UPS submodule** is also qualified per API17F and designed with A and B redundancy, allowing AC or DC power to be rerouted from one side to the other in the event of an internal component failure. The submodule is composed of transformers to adjust the incoming voltage (ranging from 110–3000 VAC) to a standardised 150–240 VAC range, aligning with typical battery charging requirements, and a power factor controller stabilising the output voltage to 400 VDC delivered to the DC-FO submodule. The AC&UPS unit also incorporates a suite of switches enabling the management of power flow for both charging and discharging batteries; communication with the external battery canister's Battery Management System (BMS) is achieved through the CANopen protocol.

The external **battery module** is typically a field-specific add-on designed to meet the power requirements of each deployment, with a typical capacity of 30 kWh.

## Inductive Wireless Power Transfer, Technology selection on the SDS

**Technology selection.** The outputs of the Subsea Control Module (SCM) described in Section 2.2 could theoretically be directly interfaced with a UID using a wet-mate connector, comparable to charging an electric vehicle on land. However, this approach was not pursued due to several inherent limitations of wet-mate connectors. Such connectors require precise alignment of the UID within a dynamic and often unpredictable hydrodynamic environment, presenting significant control challenges in the presence of ocean currents. Additionally, wet-mate connectors necessitate mechanisms capable of generating the necessary force for mating and demating operations. A further limitation is the finite operational lifespan of wet-mate connectors, typically constrained from 500 to 1,000 mating cycles. Given the permanent subsea installation rating of the SDS and the potential need for daily UID missions, wireless technologies were identified as a more suitable solution to ensure long-term reliability and operational efficiencies.

Among the wireless technologies available for power transfer—capacitive, inductive, radio frequency, and optical—Inductive Wireless Power Transfer (IWPT) has emerged as the most viable solution for subsea applications (Martínez de Alegría et al., 2024). IWPT is widely used in consumer electronics and EV charging, facilitating technology transfer for underwater applications. Modern IWPT systems demonstrate high power capacities and high efficiency. For instance, in applications such as high-speed trains, IWPT has been shown to achieve power transfer levels of up to 1 MW with efficiencies exceeding 82% across a 5 cm air gap (Kim et al., 2015).

In contrast, best-in-class IWPT optimised for sea conditions can achieve power transfer levels of 10 kW with an efficiency of 91% over a gap of 25 mm in an aquarium set-up (Yang et al., 2023). However, in practical operation, the inductive couplers of the SDM are rated for 2.5 kW power transfer. Commercial operation in seawater presents additional challenges, including (i) the dimensioning of coils and ensuring their compliance to standards lifetime under sustained water pressure, (ii) mitigating the increased eddy current losses caused by the salinity and conductivity of the seawater and (iii) limited power available subsea.

- i. With power electronics optimised, larger coils in an IWPT system transfer more power. However, subsea conditions impose spatial constraints not found in topside environments, limiting the deployment of large coils and, hence, power. Commercial subsea equipment, such as the SDS and its associated components, are typically rated for operation at depths of up to 3000 meters. At this depth, the hydrostatic pressure reaches 307 kgf/cm<sup>2</sup>, a 20 cm diameter coil will be subjected to a force of 96.6 metric tons. To withstand these forces, materials such as aluminium and super duplex steel are used to support the coil, adding weight. Since the same electronic system is also implemented on the UID side, where weight is a critical factor, the coil dimensions—and thus power transfer—are weight-optimised. Furthermore, as an API 17F-certified system with a 15-year lifetime requirement, the IWPT electronics, hence the rated power transfer, are de-rated to provide a lifetime margin for the equipment.
- ii. Increasing the operating frequency to operate with smaller coils is not a viable option subsea. In saline environments, the conductivity of seawater interacts with electromagnetic fields, inducing eddy currents that result in additional power losses and constraints on the operational frequency. In IWPT technologies, the efficiency of wireless power transmission  $\eta_{max}$  is fundamentally constrained by the product of the magnetic coupling factor ( $K$ ) and the inductor quality factor ( $Q$ ), as expressed by the relationship  $\eta_{max} \approx 1 - \frac{2}{KQ}$  (Bosshard et al., 2013). Optimal efficiency is achieved by maximising the product of ( $K$ ) and ( $Q$ ). While the coupling factor ( $K$ ) relates to the magnetic coupling quality between the transmitting and receiving coils; i.e. a closer spatial alignment of the coils enhances ( $K$ ), ( $Q$ ) the inductor quality factor defined as  $Q = \sqrt{Q_1 Q_2}$  ,  $Q_i \approx 2\pi f L_i / R_{ac,i}$  (where

$f$  denotes the operating frequency,  $L$  represents the coil inductance and  $R_{ac,i}$  is the AC resistance at  $f$  shows that high frequencies improve ( $Q$ ). However, as the conductivity of seawater induces eddy currents, high operational frequencies reduce the quality factor ( $Q$ ) of the inductor in seawater. Prakash (Prakash et al., 2016) analysed optimal frequency ranges for wireless power transmission in saline conditions and identified 75 to 125 kHz as the most effective window. Maintaining a high power transfer efficiency in a subsea context is critical as energy losses generate heat that accelerates the delamination of the coil's protective encapsulation, leading to potential water ingress and system failure over the 15-year operational lifetime requirement.

- iii. Subsea fields operate with limited power availability. State-of-the-art Direct Current Fiber Optic (DC-FO) systems typically provide 2.5 kW per access point, whereas older brownfield installations may supply only up to 1 kW. These constraints are further compounded by step-out distances spanning several kilometres, which result in substantial voltage drops along the transmission line. Consequently, the power available at the cable's termination can be severely restricted, emphasising the need for appropriate wireless power transfer solutions up and onboard energy storage solutions.

Due to the operational and fundamental constraints outlined above, as well as adherence to established standards, a planar coil topology operating in close coupling at 100 kHz with a power transfer capacity of 2.5 kW has been selected as the primary mode for recharging UIDs. Modern work-class UIDs are typically equipped with battery packs ranging from 20 to 80 kWh, meaning a full charge will require between 8 and 32 hours. Time of charge is currently a limited concern as there is typically waiting time in between missions. Furthermore, the inductive couplers support load-sharing, enabling two or more couplers to operate simultaneously to deliver a combined charging capacity of  $2.5\text{kW} \times n$ , where  $n$  is the number of 2.5 kW inductive couplers used simultaneously. Additionally, as the UID collects data during operation, the inductive charging system has been designed with integrated communication capabilities to enable data transfer, full duplex, at a speed of 100 Mbps while charging.

Auxiliary inductive couplers, available in 250 W or 350 W configurations and utilising the same core technology are also integrated into the SDM, however those are used to power sensors or to create tether links with UIDs. The following section focuses on the 2.5 kW primary chargers, while section 4 highlights the benefit of auxiliary 250/350W inductive couplers.

***Integration of 2.5 kW inductive technology on the SDM for recharging UIDs.*** As illustrated in Fig. 7, the SDM hosts the inductive couplers. The 2.5 kW primary inductive coupler (Tx), responsible for transmitting power, data, and positioning signals, is fabricated from duplex material and permanently housed within the SDM. The secondary coupler (Rx), which receives the transmitted power and data, is integrated into the UID. In this specific case, the couplers are bidirectional, meaning they can both transmit and receive power and data. However, the terms Tx and Rx are used here as a naming convention for clarity. Together, the 2.5 kW inductive coupler system enables the transfer of power, data, and relative positioning information across a water gap of up to 10 mm, providing the necessary flexibility for subsea landing operations.

The primary, powered by an input voltage of 400 VDC, incorporates an inverter, a control system, and a compensation network. The secondary module features rectification and control networks designed to deliver stable and maximum power to the load, such as batteries, during both transient and steady states. Wireless energy transfer is achieved through mutually inductive coupling in the near field at or near the resonance frequency, while critical control information is transmitted simultaneously via the regulation channel (see Fig. 8). To enable high-speed data transmission, the coupler integrates an additional 2.4 GHz radio frequency carrier, which provides a full-duplex 100 Mbps bandwidth surpassing acoustic methods and avoids the line-of-sight requirements of optical links (Qureshi et al., 2016).

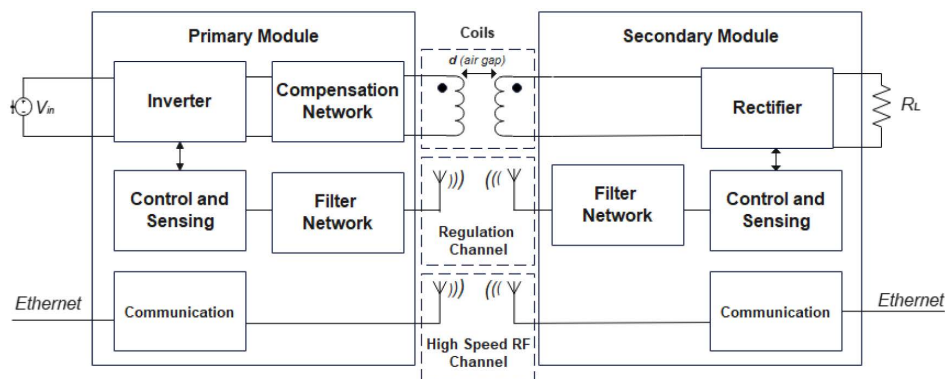


Figure 8—2.5 kW Rx and Tx inductive coupler block diagram

To enhance the power transfer in the 2.5 kW inductive coupler, a series-parallel (SN) topology is employed, leveraging the load independence and straightforward design—benefits also highlighted for electric vehicle (EV) applications (Rahulkumar et al., 2023) (Zhang et al., 2019). Such a network mitigates large reactive components caused by low mutual inductance and reduced coil coupling factors (Feliziani et al., 2024), matching system impedance and eliminating voltage-current phase differences to improve power transfer efficiency (Panchal et al., 2018).

Control is pivotal for stable and efficient power delivery; Fig. 9 shows the inductive coupler control system. This system features an H-bridge inverter operating under an SN topology, where the capacitor and coil are in series on the primary side. The H-bridge itself comprises four MOSFETs (Q1, Q2, Q3, and Q4), which support nine possible switching modes. In a half-bridge configuration, only one leg (for example, Q1 and Q2) is driven by complementary control signals, while the other leg remains inactive, yielding a unipolar output. In a full-bridge configuration, both legs are active, producing a bi-polar output – for instance, by powering the diagonal pairs Q1 and Q4 or Q2 and Q3. These flexible switching strategies enable precise management of power flow to accommodate various operational subsea load requirements.

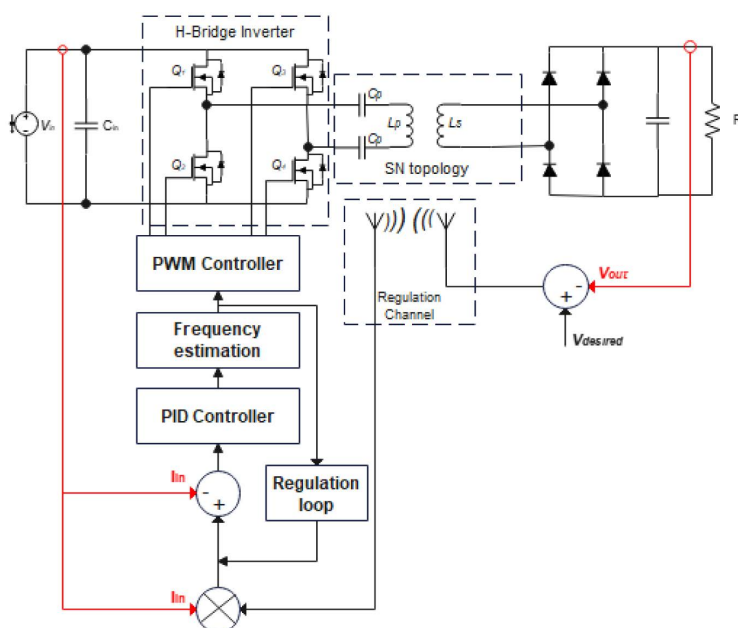


Figure 9—2.5 kW Rx and Tx Inductive coupler control system

The SN compensation network achieves optimal energy transfer at the resonance frequency. Under the control architecture, the frequency of operation initially starts above resonance and then shifts toward the

resonant point based on load requirements. Within this system, the desired voltage on the secondary side serves as the setpoint and is transmitted to the primary through the regulation channel. A PID controller processes this signal, and its output is subsequently fed into a frequency estimation stage. This stage then determines the appropriate switching mode and frequency needed to maintain the target voltage and ensure efficient power delivery. In addition, optimised regulation, power electronics, and coil design enable this approach to deliver high efficiency > 90% at all loads above 500W, as shown in Fig 10.

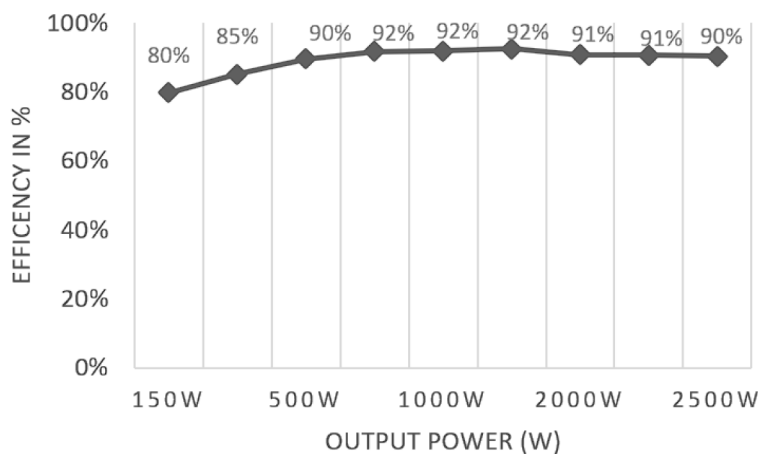


Figure 10—Wireless power transmission efficiency of the 2.5 kW inductive coupler as a function of the load

Besides high efficiency, the inductive coupler also incorporates advanced battery management capabilities through constant current (CC) and constant voltage (CV) charging algorithms. Its high configurability enables on-the-fly adjustments without requiring hardware modifications, allowing it to function as a controllable power supply and battery charger. Soft-start protection mitigates damage risks during transient conditions, while rapid load regulation ensures system stability in response to current fluctuations. The inductive coils, galvanically isolated from each other, function as a 1:1 transformer, enhancing safety and system design simplicity.

The inductive coupler, in addition to facilitating bidirectional reliable power and data transfer, also plays a critical role in enabling precise navigation and docking of UIDs, achieving millimeter-level positional accuracy. Unlike funnel-type charging stations, which simplify the docking process through a more straightforward design using mechanical guiding, the flat landing plate configuration of the SDS introduces additional complexity in both (i) securing of the drone and (ii) landing. The inductive coupler described herein has been specifically engineered to address these dual requirements, ensuring both accurate positioning and secure docking. In the oil and gas sector, hovering-type UIDs are extensively employed for detailed close-range inspections of complex and intricate structures. These advanced systems are integrated with sophisticated sensors, significantly limiting the feasibility of employing mechanical guidance mechanisms.

- i. The primary-side connector is equipped with a locking mechanism, such as a "click-lock" or an actively operated gripper system, to securely interface with the docking structure (see Fig. 16)
- ii. UID docking is achieved through a multi-stage process integrating sonar terrain navigation, acoustic communication, machine vision on optical markers, and magnetic field triangulation. Initially, sonar and acoustic signals guide the UID to within a 10-meter radius of SDS. Upon reaching this proximity, optical communication is established, the UID onboard camera detects the Aruco markers on the SDS enabling both identification and rough positioning. When the UID is within one meter of the docking platform, the primary coupler generates a magnetic field (see Fig. 11), which is detected by inductive magnetic sensors embedded in the secondary coupler. These sensors, arranged at

120° intervals, deliver highly accurate positional feedback, enabling millimeter-level precision in the horizontal plane (i.e., X and Z coordinates). Concurrently, the voltage intensity detected by the secondary coil provides positional information in the vertical plane (i.e., Y coordinate). This integrated system allows the UID to determine its position within a three-dimensional X, Y, Z reference frame, with the origin defined at the location of the primary inductive coupler.

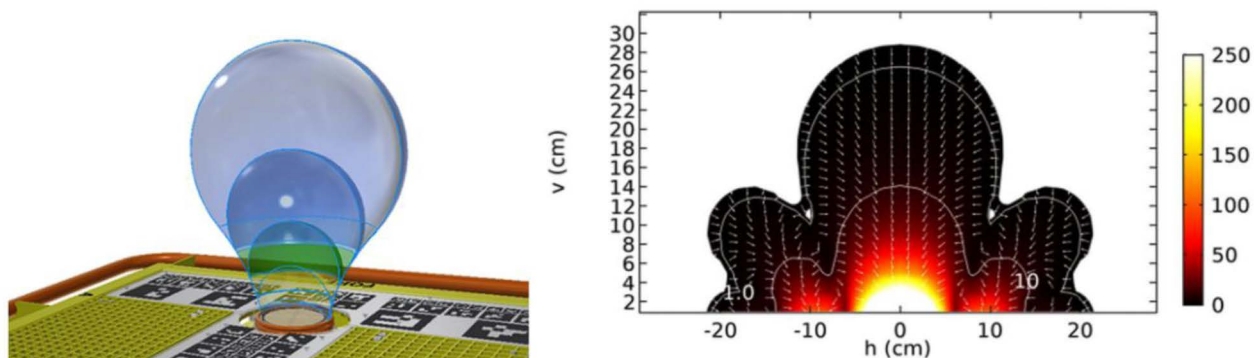


Figure 11—(left) Visualisation of the primary side's magnetic field, allowing precise UID docking within a millimetre accuracy (right) voltage induced in the secondary coil. The area where the induced voltage is above 1 V is shown.

## Role of the SWiG Standard in Ensuring Compatibility

Established in 2011, the Subsea Wireless Group (SWiG) aims to promote interoperability and interchangeability for subsea wireless communications. SWiG is an effective vehicle for standardisation as it encompasses representatives from the entire supply chain – end-user operators, integrators and technology vendors, which means that resultant standards created by the group are broadly acceptable to the whole supply chain. Current members of SWiG are shown in Fig. 12.



Figure 12—Current SWiG members encompassing end-user operators, integrators and technology vendors

Due to the complexity of underwater communications, which involve a wide range of distinct technologies such as radio frequency communication, acoustic communication, optical communication, inductive power and data transfer, as well as the eventual goal of enabling seamless hybrid systems, multiple standards are being developed under the SWiG framework. The process of finalising these multiple standards is currently underway.

The SWiG Standard serves as a unifying framework, acting as an umbrella for a constellation of technology-specific standards, including radio, acoustic, optical, inductive, and hybrid communication

methods. Its primary objective is to ensure compatibility and interoperability across these diverse technologies by establishing a standardised interface for communicating with subsea equipment. While the mechanical details of this interface are not yet fully defined, the communication methodology has been clearly specified; the SWiG Standard defines data elements, system capabilities, and operational sequences, creating a cohesive foundation for subsea communication. Additionally, it specifies the serialisation of data and the protocols required for encoding and decoding across various physical media (see Fig. 13). This unified approach simplifies communication, enabling a generalised, vendor-neutral framework that facilitates seamless interoperability among subsea devices from different manufacturers.

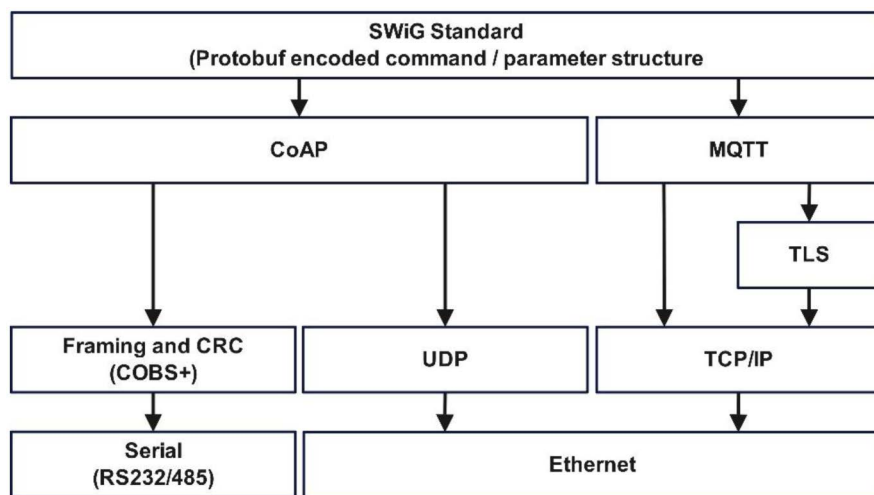


Figure 13—Currently envisaged SWiG Standard protocol format with Protobuf over different interfaces and protocols. UDP: User Datagram Protocol, TCP/PI: Transmission Control Protocol/Internet Protocol, Tls: Transport Layer Security, CRC: Cyclic Redundancy Check, CoAP: Constrained Application Protocol, MQTT: Message Queuing Telemetry Transport

In the case of a subsea inductive coupler, as discussed in Section 2, the SWiG Standard governs the dry interface, which connects the inductive coupler to the topside network via the SCM. Meanwhile, the SWiG Inductive standard specifically addresses the wet interface, which facilitates the connection between the primary and secondary sides of the inductive coupler (See. Fig 14).

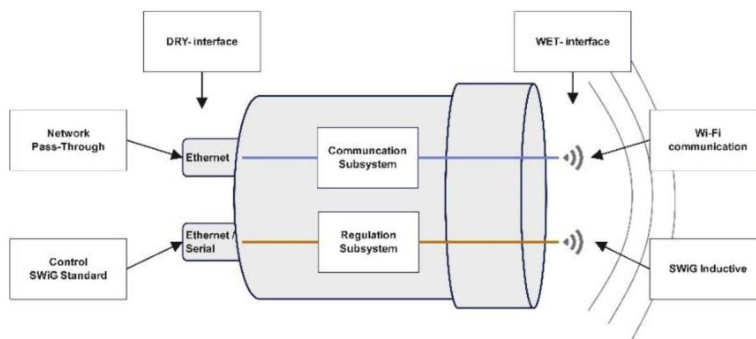


Figure 14—Differentiation between SWiG Standard addressing the dry interface and SWiG Inductive covering the Tx-Rx interface

The SWiG Inductive, the inductive data and power standard, defines the (1) physical characteristics of couplers, i.e. size and mechanical interface, (2) the communication protocols and (3) power regulation mechanisms between inductive connectors. The standard enables seamless integration, allowing devices, Tx or Rx, from different vendors to be paired and interchanged.

The inductive standard encompasses both power transfer and one or more communication channels, with its capabilities and physical properties classified into the following categories: (a) Type and Shape, (b) Communication Coil Size and Capacity, (c) Power Coil Size and Capacity, (d) Separation Distance. These classifications govern mechanical envelope sizes and capabilities for pairing a transmitter and a receiver. For example, the SWiG-compatible inductive couplers described in sections 2 and 4 are defined as <F45-140-782> for the 2.5kW and <F30-80-481> for the 350W; the coding corresponds to type/shape/communication coil size/power coil capacity/communication capacity and separation capacity.

The following section provides an overview of the SWiG inductive power protocol. It details the operational steps undertaken by a SWiG-compatible inductive device to ensure seamless functionality across vendors, focusing on the (i) handshake and (ii) regulation processes.

- i. Handshake process: SWiG-compatible inductive devices initially operate in an "Object Detection" (OB) state, during which they monitor for nearby devices while providing a protective mechanism against foreign objects. The OB state detects the presence of external influences on the magnetic field without initiating communication, ensuring operational safety and efficiency. Once two devices detect each other, they transition into a pairing mode, during which a handshake process is performed. This handshake comprises the following sub-phases:
  - a. Version compatibility and matching confirm that both devices adhere to compatible protocol versions, ensuring interoperability.
  - b. Static information exchange transfers device-specific, exchanging data to establish a baseline for communication.
  - c. Dynamic information exchange shares real-time, operationally relevant data such as adjustable power configuration between devices.
  - d. Link quality test assesses the reliability and robustness of the communication channel.

Vendor information is exchanged early in the handshake process to accommodate vendor-specific extensions while preserving the protocol's flexibility and scalability.

- ii. Regulation process: The SWiG inductive protocol emphasises vendor independence and optimal regulation efficiency by minimising feedback loop delay. This is achieved through high-speed data transmission at intervals of 1/2000th of a second using a lightweight binary format. A unique feature of the protocol is its early encoding of the feedback regulation value within the data packet, along with a dedicated redundancy check. This allows the decoder to validate and apply the offset value even before the full data packet is received, enabling faster response times and improved system performance.

Beyond feedback regulation, the protocol supports the transmission of Tag/Value pairs to enable continuous updates on device status, alarm notifications, control signals, and condition monitoring. Unlike traditional request/response mechanisms, this protocol employs a "send-and-forget" approach, where each information element is transmitted at a defined frequency within the 2,000 packets per second stream. This ensures efficient channel utilisation and reliable, timely delivery of critical data.

## Case Study: Deployment at Njord Field

Equinor deployed the Hydrone-R combined with an SDS at Njord Field (see [Fig. 15](#)) in 2022-2023 ([Eriksen Trond, 2024](#)) as part of its strategy to enhance underwater intervention capabilities ([Torvestad, 2018](#)). Prior to the deployment at Njord, the Hydrone-R underwent 4700 hours of sea trials and 2000 hours of continuous dive testing, validating the system's reliability ([Cavallini Francesco, 2024](#)).

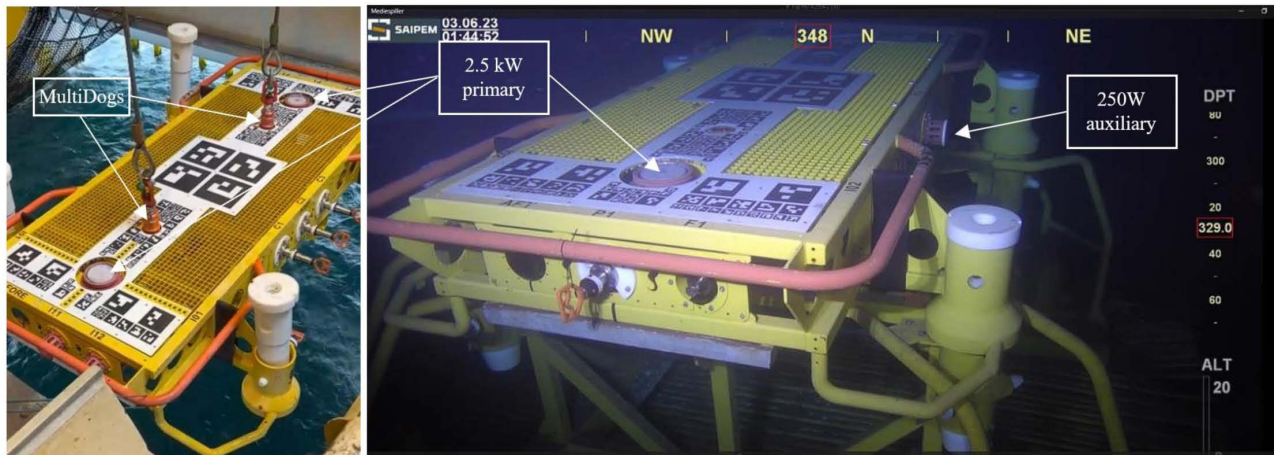


Figure 15—(left) installation of the SDM at Njord via the moonpool, (right) SDM on the gravity base structure installed at -329-meter seawater

In 2023, the Hydrone-R completed a 165-day uninterrupted dive, setting a world record for autonomous underwater operations with over 280 successful docking and undocking cycles (see Fig. 16), demonstrating the robustness of the SDS interface.



Figure 16—(left) Hydrone R approaching the SDS, guided by magnetic fields emitted by the 2.5 kW inductive coupler; (right) Hydrone R securely docked to the SDS, with the gripper mechanism anchoring the drone to the 2.5 kW inductive primary coupler

The most valuable outcome of the mission was the successful execution of 35 precise manipulations by the drone, including valve operations, demonstrating its precision and versatility. A significant portion of critical missions were conducted when the drone self-tethered itself to the charging station via the auxiliary 250 W, 100 Mbps data inductive coupler (see Fig. 17).

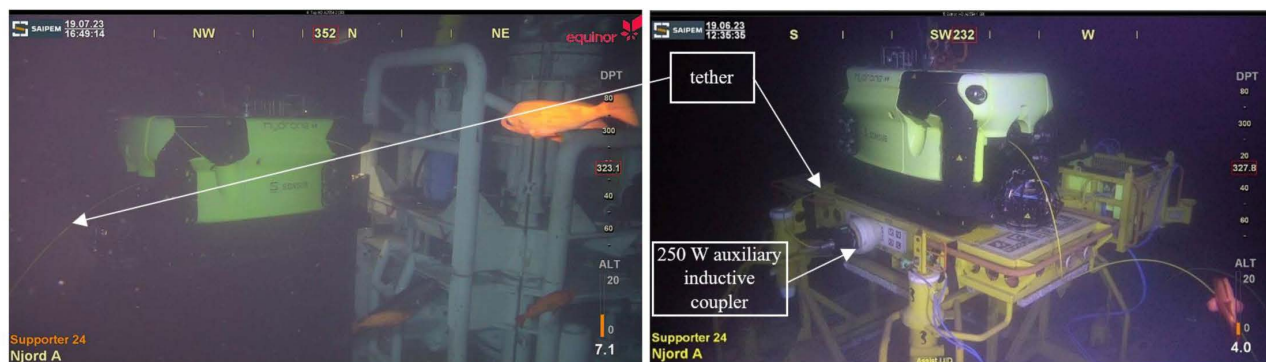


Figure 17—(left) Hydroner R tethered to the SDS operating as an ROV, (right) tether connection point on the SDM facilitated via the 250 W induction module.

This setup enabled the drone's real-time control, i.e. <math><100\text{ms}</math> latency, from the offshore control centre in Stavanger or the Njord rig centre. The ability to seamlessly transition between AUV inspection mode and ROV mode, facilitated by the tether-auxiliary inductive coupler combination, significantly enhanced the operational flexibility and economic viability of resident drones. In the case of the Hydroner-R, the tether system included a spool with a range of 300 meters.

## Expanding Applications Beyond Oil and Gas

Although the O&G industry is a market driver in the utilisation of large UIDs, the market of small subsea drones is expanding at a fast pace. Sudmann in (Sudmann, 2023) addresses limitations of small AUVs that require tethered connections or frequent resurfacing for battery swapping by re-using the inductive technology used in the SDS to create a docking station for small underwater drones. To meet the requirements of the small AUV market, the steel super duplex housing of the 250W auxiliary inductive coupler has been replaced with a design integrating the power electronics and coil within a polyurethane mould. This optimisation has resulted in a compact ( $\text{\O}11\text{ cm}$ , height 3.6 cm), lightweight (400 g in water) inductive coupler. The redesigned system is de-rated for operation at depths of up to 400 meters; however, it maintains a power transfer capacity of 250W and data transfer rates of up to 100 Mbps, all while being cost-efficient (see Fig. 18).

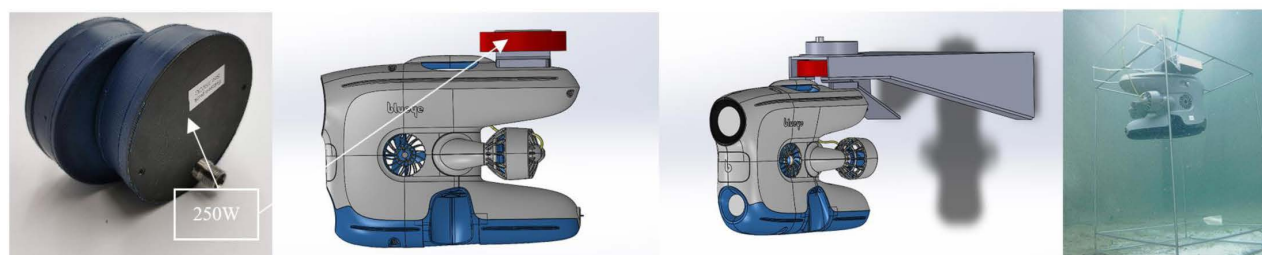


Figure 18—Sudmann funnel charging station concept for small UID, the red disk is the redesigned SDS's auxiliary 250W inductive coupler

Employing a buoyancy-based docking concept, the station of Sudmann integrates a funnel mechanism for alignment and a fin-mounted 250W inductive coupler combined with magnetic grips to enable wireless charging and data transfer (Fig. 18). Compatibility with the Blueye X3 ROV was prioritised during development. However, the system is adaptable to other small AUVs. The design of the docking station is simple and minimises moving parts to reduce costs, maintenance and ensure long-term reliability. During the 25 trials with the Blueye X3, the drone successfully docked every time, validating the station concept.

A crucial component of any resident AUV system is the development of a navigation system capable of autonomous docking. Moslåttn in (Moslåttn B. M., 2024) investigated a system that fuses monocular visual odometry, enhanced by fiducial markers, with velocity and acceleration data from an Inertial Measurement Unit (IMU) and a Doppler Velocity Log (DVL) to produce accurate and robust pose and velocity estimates (see Fig.19). As part of the MarTERA UNDINA project, the system proved its robustness and reliability by successfully performing numerous consecutive autonomous dockings under various initial conditions. These results mark another significant step toward the feasibility of one-person portable vehicles for subsea residency and long-term operations.



Figure 19—Docking station equipped with fiducial markers and funnel charging. The vehicle performs autonomous docking manoeuvres from Moslåttn.

Using the same 400m rated 250W inductive technology and adding visual markers for autonomous docking, the company Hydromea within the Eurostar REDRA project 2171 created a compact docking station for the EXRAY drone (Fig. 20). This system enables the AUV to remain resident within its operational environment ensuring uninterrupted data collection and extended deployment. Through the docking station, the AUV can be charged up to 90% of its capacity in 2 hours and at full capacity in 3 hours. Moreover, the station provides continuous telemetry of the charging status to accurately estimate the state-of-charge (SoC) of the batteries and remote monitoring of the charging process.

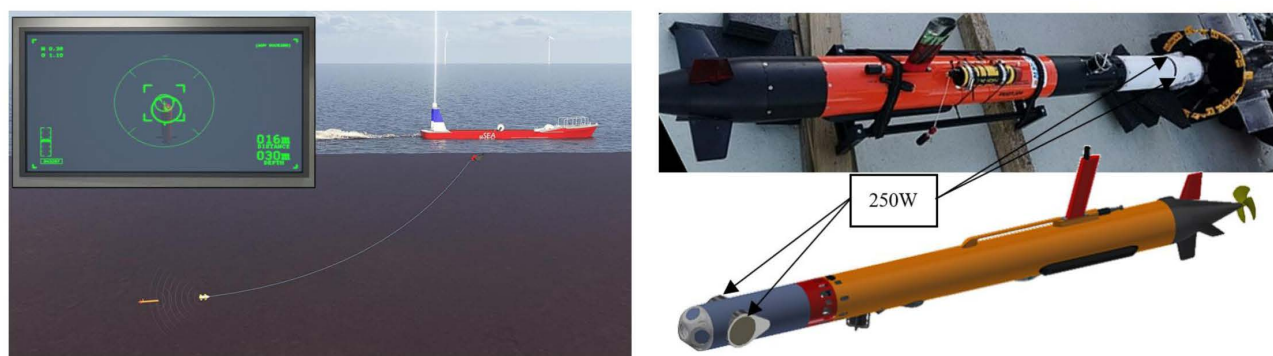


Figure 20—Hydromea charging station concept for the EXRAY using the same inductive technology used in Sudmann, 2023 and Moslåttn (2024).

REDRA key application is in aquaculture, where the resident drone autonomously monitors fish pens and provides daily comprehensive reports. These reports shall include water quality metrics such as salinity, temperature, oxygen levels, and chlorophyll content; net condition assessments, especially post-storm; and continuous monitoring of fish health using onboard sensors.

An interesting alternative to classic seabed-resident AUV systems is being investigated in the ACCESS-AUV project coordinated by USEA Ocean Data. A novel active towed docking station with power and data transfer capabilities has been developed to enable AUV operations from unmanned surface vessels (USVs) without the need for surfacing or physical recovery. This approach allows operations in a broader

range of weather and sea conditions. The technology enables wireless power transfer (charging) and high-speed data exchange between the towed docking station and the AUV while it remains submerged and in motion (see Fig 21). The wireless inductive connectors installed in the OceanScan MST LAUV's nose also stem from the same technology used in the SDS 250W auxiliary inductive couplers; however, two are used simultaneously to deliver 500W. While docked and towed, the AUV charges upload the latest mission logs and data and download new mission plans simultaneously. USEA, in collaboration with NTNU, tested the docking system at depths ranging from 7 to 30 meters in sea states 3-4, with little to no impact on system performance.



**Figure 21—(left) Towed docking station concept (right) the modified nose of an AUV with 2x 250 W inductive connectors and communication antennas installed at the front. Courtesy of USEA**

These examples illustrate just a fraction of the potential cross-market application of the inductive technology used in the SDS. While the oil and gas industry remains a primary driver for large UIDs, the rapid expansion of the market for smaller subsea drones highlights the adaptability of this innovation. From buoyancy-based docking stations for compact AUVs to towed systems, the subsea IWPT is being adapted to meet diverse operational challenges.

## Conclusion and Future Prospects

This paper demonstrates that when integrated into standardised subsea docking stations, wireless inductive charging technology serves as a cornerstone for enabling autonomous and resident underwater operations. The results presented, particularly the 165-day uninterrupted deployment of the Hydrone-R in Equinor's Njord Field, underscore this approach's robustness, economic viability, and environmental benefits. The ability to dock 280 times, conduct 35 precision manipulations without surface vessel highlights SDS technology as a solution for reducing operational costs and carbon emissions in offshore industries.

Key enablers of this success include the modularity and open innovation model of the SDS, which supports multiple underwater intervention drone types combined with the SWiG-compliant inductive charging technology, which ensures charging interoperability across manufacturers. These features position the SDS as an industry-leading infrastructure capable of adapting to diverse operational demands. Beyond the oil and gas sector, the adoption of smaller-scale inductive docking stations in aquaculture and environmental monitoring illustrates the versatility of this innovation.

Looking ahead, the continued evolution of subsea technology will require addressing certain limitations. Increasing inductive power transfer capabilities beyond the current 2.5 kW to at least 5–10 kW and scaling data transfer rates to 1 Gbps or higher will support the growing needs of larger UIDs with 100 kWh battery packs and more data-intensive missions. For smaller drones, lightweight, low-cost docking systems tailored to shallower depths will facilitate broader adoption in new markets.

The SDS provides a clear path toward a universal standard for subsea operations, akin to the interoperability of terrestrial refuelling stations. However, realising this vision will require greater

collaboration across industries to further refine SWiG standards and promote their adoption globally. By fostering open innovation and maintaining interoperability, the SDS has the potential to become the backbone of a fully integrated, cost-efficient, and environmentally sustainable subsea ecosystem.

## List of abbreviations

Abbreviation	Meaning
AC	Alternating Current
ACCESS	Active Towed Docking Station Project
API	American Petroleum Institute
AUV	Autonomous Underwater Vehicle
BMS	Battery Management System
BP	British Petroleum
CAD	Computer-Aided Design
CAN	Controller Area Network
CC	Constant Current
CO2	Carbon Dioxide
CRC	Cyclic Redundancy Check
CV	Constant Voltage
DC	Direct Current
DC-FO	Direct Current Fiber Optic
DNV	Det Norske Veritas
DSV	Diving Support Vessel
DVL	Doppler Velocity Log
EV	Electric Vehicle
EXRAY	Subsea Drone Name in Eurostar Project
FO	Fiber Optic
IMR	Inspection, Maintenance, and Repair
IMU	Inertial Measurement Unit
IWPT	Inductive Wireless Power Transfer
LAUV	Light Autonomous Underwater Vehicle
MQTT	Message Queuing Telemetry Transport
MST	Marine Subsea Technologies
Mbps	Megabits per second
MW	Megawatt
NORCE	Norwegian Research Center
NTNU	Norwegian University of Science & Technology
OB	Object Detection State
OTC	Offshore Technology Conference
PI	Proportional-Integral
PID	Proportional-Integral-Derivative

Abbreviation	Meaning
REDRA	Eurostar REDRA Project
ROV	Remotely Operated Vehicle
SCM	Subsea Control Module
SDB	Subsea Docking Base
SDM	Subsea Docking Module
SDS	Subsea Docking Station
SN	Series-None (topology)
SPS	Subsea Production System
SWG	Subsea Wireless Interface Group
TCP	Transmission Control Protocol
TR1231	Equinor Technical Requirement Document
UDP	User Datagram Protocol
UID	Underwater Intervention Drone
UNDINA	MarTERA UNDINA Project
UPS	Uninterruptible Power Supply
USB	Universal Serial Bus
VAC	Volts Alternating Current
VDC	Volts Direct Current

## References

- API 17F. (2023). *Standard for Subsea Production and Processing Control Systems*.
- Ariana Hurtado. (2021). OTC 2021: Saipem develops resident subsea drone. *Offshore*. <https://www.offshore-mag.com/subsea/article/14208737/otc-2021-saipem-develops-resident-subsea-drone>
- Bosshard, R., Mühlethaler, J., Kolar, J. W., & Stevanovic, I. (2013, March). Optimized magnetic design for inductive power transfer coils. APEC 2013: Twenty-Eighth Annual IEEE Applied Power Electronics Conference and Exposition.
- Cavallini Francesco. (2024). An underwater robotics milestone: commissioning & start-up of UID operations at Njord subsea forum-Digital Twins, Data Acquisition, AI. *Presentation at AOG Energy*.
- Elaine Maslin. (2021). Subsea Vehicles: To Be (Resident), Or Not To Be? *Marine Technology*. <https://www.marinetechologynews.com/news/subsea-vehicles-resident-614272>
- Eriksen Trond. (2024). Implementation process of UID, Hydrone-R at Njord A. *FFU Seminar*.
- Feliziani, M., Campi, T., Cruciani, S., & Maradei, F. (2024). Compensation networks of automotive WPT system. *Wireless Power Transfer for E-Mobility*, 185–220. <https://doi.org/10.1016/B978-0-323-99523-8.00002-3>
- Hurtado, A. (2023). Executive insights: Remote operations are evolving with ROV/AUV advancements Oceanengineering executive details the challenges and solutions of remote operations. *Offshore*. <https://www.offshore-mag.com/subsea/article/14293585/oceanengineering-executive-insights-remote-operations-are-evolving-with-rov-auv-advancem...>
- Kim, J. H., Lee, B. S., Lee, J. H., Lee, S. H., Park, C. B., Jung, S. M., Lee, S. G., Yi, K. P., & Baek, J. (2015). Development of 1-MW Inductive Power Transfer System for a High-Speed Train. *IEEE Transactions on Industrial Electronics*, 62(10), 6242–6250. <https://doi.org/10.1109/TIE.2015.2417122>
- Magnus Valen. (2010). *Launch and recovery of ROV: Investigation of operational limit from DNV Recommended Practices and time domain simulations in SIMO* [NTNU]. [https://ntnuopen.ntnu.no/ntnu-xmlui/bitstream/handle/11250/237839/375590\\_FULLTEXT01.pdf?sequence=1&isAllowed=y](https://ntnuopen.ntnu.no/ntnu-xmlui/bitstream/handle/11250/237839/375590_FULLTEXT01.pdf?sequence=1&isAllowed=y)
- Martínez de Alegría, I., Rozas Holgado, I., Ibarra, E., Robles, E., & Martín, J. L. (2024). Wireless Power Transfer for Unmanned Underwater Vehicles: Technologies, Challenges and Applications. In *Energies* (Vol. 17, Issue 10). Multidisciplinary Digital Publishing Institute (MDPI). <https://doi.org/10.3390/en17102305>
- Martyn Wingrov. (2023). *Riviera - News Content Hub - OSV charter rates to break records in 2024*. [https://www.rivieramm.com/news-content-hub/news-content-hub/sold-out-market-drives-rates-to-eight-year-high-79195?utm\\_source=chatgpt.com](https://www.rivieramm.com/news-content-hub/news-content-hub/sold-out-market-drives-rates-to-eight-year-high-79195?utm_source=chatgpt.com)

- Moslått B. M. (2024). *Guidance, Navigation and Control System for Autonomous Docking of Unmanned Underwater Vehicles*. NTNU.
- Panchal, C., Stegen, S., & Lu, J. (2018). Review of static and dynamic wireless electric vehicle charging system. *Engineering Science and Technology, an International Journal*, **21**(5), 922–937. <https://doi.org/10.1016/J.JESTCH.2018.06.015>
- Pimentel, J., & Kristiansen, K. (2022). UID™ Docking Station Control and Power Distribution System. *Norwegian Society of Electric and Automatic Control*.
- Prakash, D., Arunachalam, V. U., Narayanaswamy, V., Arumugam, V., Raju, R., Ananda, G., Malayath, R., & Atmanand, A. (2016). Analysis of Subsea Inductive Power Transfer Performances Using Planar Coils. *Marine Technology Society Journal*, **50**(1).
- Qureshi, U. M., Aziz, Z., Shaikh, F. K., Aziz, Z., Shah, S. M. Z. S., Shah, S. M. Z. S., Sheikh, A. A., Felemban, E., & Qaisar, S. Bin. (2016). RF path and absorption loss estimation for underwater wireless sensor networks in different water environments. *Sensors (Switzerland)*, **16**(6). <https://doi.org/10.3390/s16060890>
- Rahulkumar, Narayanamoorthi, Pradeep, Balaji, Gono, Dockal, Gono, & Krejci. (2023). A review on resonant inductive coupling pad design for wireless electric vehicle charging application. *Energy Reports*, **10**, 2047–2079. <https://doi.org/10.1016/J.EGYR.2023.08.067>
- Sirevaag, R., & Rettedal, A. (2021). *TRI231 Appendix D UID Subsea Docking Station requirements Management system Requirements, TRI231 Appendix D, Version 1.0*.
- Sudmann, S. (2023). *Design and Prototyping of a Universal Docking Station for Small Underwater Vehicles*. Institutt for marin teknikk.
- Tillin, H. M. (2018). *Marine monitoring platform guidelines: Remotely Operated Vehicles for use in marine benthic monitoring*. Peterborough: Joint Nature Conservation Committee. <https://noc.ac.uk/>
- Torvestad, J. C. (2018). *UID Subsea Docking Station*.
- Vasilijevic, A., Barstein, K., & Bremnes, J. E. (2023). Infrastructure for remote experimentation in the Trondheim fjord. *OCEANS 2023 - Limerick, OCEANS Limerick 2023*. <https://doi.org/10.1109/OCEANSLimerick52467.2023.10244448>
- Yang, L., Li, X., Zhang, Y., Feng, B., Yang, T., Wen, H., Tian, J., Zhu, D., Huang, J., Zhang, A., & Tong, X. (2023). A review of underwater inductive wireless power transfer system. In *IET Power Electronics* (Vol. **17**, Issue 8, pp. 894–905). John Wiley and Sons Inc. <https://doi.org/10.1049/pel2.12456>
- Zhang, Y., Kan, T., Yan, Z., Mao, Y., Wu, Z., & Mi, C. C. (2019). Modeling and Analysis of Series-None Compensation for Wireless Power Transfer Systems with a Strong Coupling. *IEEE Transactions on Power Electronics*, **34**(2), 1209–1215. <https://doi.org/10.1109/TPEL.2018.2835307>